

---

# CausalBench: A Large-scale Benchmark for Network Inference from Single-cell Perturbation Data

---

Mathieu Chevalley<sup>1,2</sup> Yusuf H Roohani<sup>1,3</sup> Arash Mehrjou<sup>1</sup>  
Jure Leskovec<sup>3</sup> Patrick Schwab<sup>1</sup>  
<sup>1</sup>GSK.ai <sup>2</sup>ETH Zürich <sup>3</sup>Stanford University

## Abstract

Causal inference is a vital aspect of multiple scientific disciplines and is routinely applied to high-impact applications such as medicine. However, evaluating the performance of causal inference methods in real-world environments is challenging due to the need for observations under both interventional and control conditions. Traditional evaluations conducted on synthetic datasets do not reflect the performance in real-world systems. To address this, we introduce CausalBench, a benchmark suite for evaluating network inference methods on real-world interventional data from large-scale single-cell perturbation experiments. CausalBench incorporates biologically-motivated performance metrics, including new distribution-based interventional metrics. A systematic evaluation of state-of-the-art causal inference methods using our CausalBench suite highlights how poor scalability of current methods limits performance. Moreover, methods that use interventional information do not outperform those that only use observational data, contrary to what is observed on synthetic benchmarks. Thus, CausalBench opens new avenues in causal network inference research and provides a principled and reliable way to track progress in leveraging real-world interventional data.

## 1 Introduction

Causal inference is central to a number of disciplines including science, engineering, medicine and the social sciences. Causal inference methods are routinely applied to high-impact applications such as interpreting results from clinical trials [Farmer et al., 2018], studying the links between human behavior and economic activity [Baum-Snow and Ferreira, 2015], optimizing complex engineering systems, and identifying optimal policy choices to enhance public health [Joffe et al., 2012]. However, evaluating these methods in real-world environments poses a significant challenge due to the time, cost, and ethical considerations associated with large-scale interventions under both interventional and control conditions. Consequently, most algorithmic development in the field has traditionally relied on synthetic datasets for evaluating causal inference approaches. Nevertheless, previous work [Gentzel et al., 2019] has shown that such evaluations do not provide sufficient information on whether these methods generalize to real-world systems.

Recent advancements in high-throughput biological experimentation have created real-world systems where large-scale interventions are feasible along with a directly observable comprehensive phenotypic readout (Dixit et al. [2016], Datlinger et al. [2017, 2021]). These datasets, which capture gene expression changes following interventions to individual cells, can serve as a valuable resource for evaluating the performance of observational and interventional approaches to causal inference on real-world data. Moreover, understanding the causal relationships between the expression of genes and constructing gene regulatory networks (GRNs) can also have a profound impact on therapeutic design and drug efficacy Nelson et al. [2015], Yu et al. [2004], Chai et al. [2014], Akers and Murali [2021], Hu et al. [2020]. However, effectively utilizing such datasets remains challenging,

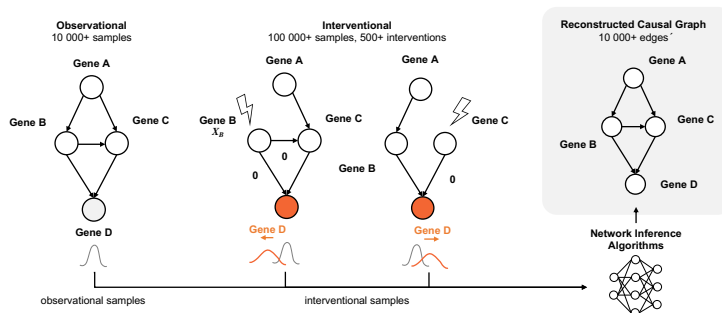


Figure 1: An overview of causal gene–gene network inference in mixed observational and perturbational single-cell data. The causal generative process in its unperturbed form is observed in the observational data (left; 10 000+ samples in CausalBench) while data under genetic interventions (e.g. CRISPR knockouts) are observed in the interventional data (right; 200 000+ samples in CausalBench). Either observational or interventional plus observational data that were sampled from the true causal generative process (bottom distributions) can be used by network inference algorithms (bottom right) to infer a reconstructed causal graph (top right) that should as closely as possible recapitulate the original underlying functional gene–gene interactions.

as establishing a causal ground truth for evaluating and comparing graphical network inference methods is difficult (Neal et al. [2020], Shimoni et al. [2018], Parikh et al. [2022]). Furthermore, there is a need for systematic and well-validated benchmarks to objectively compare methods that aim to advance the causal interpretation of real-world interventional datasets while moving beyond reductionist (semi-)synthetic experiments.

To facilitate the advancement of machine learning methods in this challenging domain, we introduce CausalBench – the largest openly available benchmark suite for evaluating network inference methods on real-world interventional data. CausalBench contains meaningful biologically-motivated performance metrics, a curated set of two large-scale perturbational single-cell RNA sequencing experiments with over 200 000 interventional samples (each of which are openly available), and integrates numerous baseline implementations of state-of-the-art methods for causal network inference. Similar to other domains, e.g. ImageNet in computer vision (Deng et al. [2009]), CausalBench can accelerate progress on large-scale real-world causal graph inference. Our benchmarking results highlight how poor scalability and inadequate utilization of the interventional data limits performance. CausalBench thus opens new research avenues and provides the necessary architecture to test future methodological developments. The source code is openly available at <https://github.com/causalbench/causalbench> under Apache 2.0 license.

**Contributions.** Our contributions are as follows:

- We introduce CausalBench – the most comprehensive benchmark suite for evaluating network inference methods using interventional data from over 400 000 interventional samples.
- We introduce a set of meaningful benchmark metrics for evaluating performance, including novel statistical metrics that leverage single-cell perturbational data to evaluate the capability of test methods in recovering strong interventional effects and minimizing the rate of omission of causal relationships.
- Using CausalBench, we conduct a comprehensive experimental evaluation of the performance of state-of-the-art network inference algorithms. This includes an analysis of performance scaling characteristics under varying numbers of training samples and intervention set sizes.
- Our results highlight an inconsistency between performance on synthetic data and real-world data. Specifically, we found that methods incorporating interventional information did not surpass observational methods, and causal methods did not outperform non-causal ones (methods not derived from causality theory). This finding underscores the necessity of benchmarks like CausalBench for providing more accurate assessments of causal methods using real-world interventional data.

## 2 Related Work

**Background.** Given an observational data distribution, several different causal networks or directed acyclic graphs (DAGs) could be shown to have generated the data. The causal networks that could equally represent the generative process of an observational data distribution are collectively referred to as the Markov equivalence class (MEC) of that DAG (Huang et al. [2018]). Interventional data offer an important tool for limiting the size of the MEC to improve the identifiability of the true underlying causal DAG [Katz et al., 2019]. In the case of gene expression data, modern gene-editing tools such as CRISPR offer a powerful mechanism for performing interventional experiments at scale by altering the expression of specific genes and observing the resulting interventional distribution across the entire transcriptome (Dixit et al. [2016], Datlinger et al. [2017, 2021]). The ability to leverage such interventional experiment data at scale could significantly improve our ability to uncover underlying causal functional relationships between genes and thereby strengthen our quantitative understanding of biology. Establishing causal links between genes can help implicate genes in biological processes causally involved in disease states and thereby open up new opportunities for therapeutic development (Mehrjou et al. [2022], Shifrut et al. [2018]).

**Network inference in mixed observational and interventional data.** Learning network structure from both observational and interventional data presents significant potential in reducing the search space over all possible causal graphs. Traditionally, this network inference problem has been solved using discrete methods such as permutation-based approaches (Wang et al. [2017], Hauser and Bühlmann [2012]). Recently, several new models have been proposed that can differentially learn causal structure (Schölkopf et al. [2021]). However, most of these models focus on observational datasets alone. Ke et al. [2019] presented the first differentiable causal learning approach using both observational and interventional data. Lopez et al. [2022] improved the scalability of differentiable causal network discovery for large, high-dimensional datasets by using factor graphs to restrict the search space, and Scherrer et al. [2021] introduced an active learning strategy for selecting interventions to optimize differentiable graph inference.

**Gene regulatory network inference.** The problem of GRN inference has been studied extensively in the bioinformatics literature in the case of observational datasets. Early work modeled this problem using a Bayesian network trained on bulk gene expression data (Friedman et al. [2000]). Subsequent papers approached this as a feature ranking problem where machine learning methods such as linear regression (Kamimoto et al. [2020]) or random forests (Huynh-Thu et al. [2010], Aibar et al. [2017]) are used to predict the expression of any one gene using the expression of all other genes. However, Pratapa et al. [2020] showed that most GRN inference methods for observational data perform quite poorly when applied to single-cell datasets due to the large size and noisiness of the data. In the case of constructing networks using interventional data, there is relatively much less work given the recent development of this experimental technology. Dixit et al. [2016] were the first to apply network inference methods to single-cell interventional datasets using linear regression.

**Benchmarks for causal discovery methods.** To benchmark new causal discovery methods, the main approach followed consists of evaluating on purely synthetic data. The true underlying graph is usually drawn from a distribution of graphs, following procedures described in Erdős et al. [1960] (Erdős-Rényi graphs) and Barabási and Albert [1999] (scale-free graphs). Given a drawn graph, a dataset is then created under an additive noise model assumption, following some functional relationship such as linear or nonlinear functions of random Fourier features. The additive noise can follow various distributions, such as Gaussian or uniform. The predicted graph is then evaluated using structural metrics that compare the prediction to the true graph. Popular metrics include precision, recall, F1, structural hamming distance (SHD) and structural intervention distance (SID) [Peters and Bühlmann, 2015]. While this type of evaluation is valuable as a first validation of a new method in a controlled setting, it is limited in its capacity to predict the transportability of a method to a real-world setting. Indeed, the generated synthetic data tend to match the assumption of the proposed method, and the complexity of their distribution is reduced and uninformedly far from the distribution of real-world empirical data. To remedy this, synthetic data generators that mimic real-world data have been proposed, such as Dibaenia and Sinha [2020] for the GRN domain. However, these simulated synthetic datasets are still limited and very reductionist, as they do not account for *unknown-unknowns* in the true data-generating process. They also still offer a large set of degrees of freedom in the choice of hyperparameters ("researcher degrees of freedom")

phenomenon [Simmons et al., 2011]). Furthermore, the distribution over the true underlying graph still needs to be chosen, and how far those generated graphs are from a realistic causal graph is also unknown. As such, Gentzel et al. [2019] thoroughly argues that the evaluation of causal methods should incorporate evaluative mechanisms that examine empirical interventional metrics as opposed to purely structural ones, and that such evaluations are best performed using real empirical data.

**Benchmarks for gene regulatory network inference** Past work has looked at benchmarking of different GRN inference approaches using single-cell gene expression data Pratapa et al. [2020]. However, this work only considers observational data and looks at small datasets of approximately 5000 samples (cells). Moreover, it does not benchmark most state-of-the-art causal inference methods.

### 3 Problem Formulation

We introduce the framework of Structural Causal Models (SCMs) to serve as a causal language for describing methods, assumptions, and limitations and to motivate the quantitative metrics. The data’s perturbational nature requires this formal statistical language beyond associations and correlations. We use the causal view as was introduced by Pearl [2009].

#### 3.1 Structural Causal Models (SCMs).

Formally, an SCM  $\mathbb{M}$  consists of a 4-tuple  $(\mathbb{U}, \mathbb{X}, \mathcal{F}, P(\mathbf{u}))$ , where  $\mathbb{U}$  is a set of unobserved (latent) variables and  $\mathbb{X}$  is the set of observed (measured) variables [Peters et al., 2017].  $\mathcal{F}$  is a set of function such that for each  $X_i \in \mathbb{X}$ ,  $X_i \leftarrow f_i(Pa_i, U_i)$ ,  $U_i \in \mathbb{U}$  and  $Pa_i \in \mathbb{X} \setminus X_i$ . The SCM induces a distribution over the observed variables  $P(\mathbf{x})$ . The variable-parent relationships can be represented in a directed graph, where each  $X_i$  is a node in the graph, and there is a directed edge between all  $Pa_i$  to  $X_i$ . The task of causal discovery can then be described as learning this graph over the variables. In the most general sense, an intervention on a variable  $X_i$  can be thought as uniformly replacing its structural assignment with a new function  $X_i \leftarrow \tilde{f}(X_{\overline{Pa_i}}, \tilde{U}_i)$ . In this work, we consider the gene perturbation as being atomic or stochastic intervention and denote an intervention on  $X_i$  as  $\sigma(X_i)$ . We can then describe the interventional distribution, denoted  $P^{\sigma(X_i)}(\mathbf{x})$ , as the distribution entailed by the modified SCM. For consistency, we denote the observational distribution as both  $P^\theta(\mathbf{x})$  and  $P(\mathbf{x})$ . This SCM framework is used throughout the paper.

#### 3.2 Problem Setting.

We consider the setting where we are given a dataset of vector samples  $\mathbf{x} \in \mathbf{R}^d$ , where  $\mathbf{x}_i$  represents the measured expression of gene  $i$  in a given cell. The goal of a graph inference method is to learn a causal graph  $\mathcal{G}$ , where each node is a single gene. The causal graph  $\mathcal{G}$  induces a distribution over observed sample  $P(\mathbf{x})$ , such that:

$$P(\mathbf{x}) = \prod p(x_i | Pa_i) \tag{1}$$

The datasets contain data sampled from  $P^\theta(\mathbf{x})$ , as well as  $P^{\sigma(X_i)}(\mathbf{x})$  for various  $i$ . The observational setting only uses samples from  $P^\theta(\mathbf{x})$ , the interventional setting includes observational and interventional data, while the partial interventional setting is a mix of the two, where only a subset of the genes are observed under perturbation.

#### 3.3 Assumptions and challenges.

Single-cell data presents idiosyncratic challenges that may break the common assumptions of many existing methods. Apart from the high-dimensionality in terms of number of variables and large sample size, the distribution of the gene expression present a challenge as it is highly tailed at 0 for some genes (Tracy et al. [2019]). Regarding the underlying true causal graph, biological feedback loops may break the acyclicity assumption underlying the use of DAGs. In addition, different cells sampled from the same batch may not be truly independent as the cells may have interacted and influenced their states. Lastly, cells in scRNAseq experiments are measured at a fixed point in time and may therefore have been sampled at various points in their developmental trajectory or cell cycle

Table 1: High-level description of the two large-scale datasets utilized in CausalBench – characterized by high numbers of samples and intervened-on variables. Of those samples, after stratification by intervention target (including no target), 20% were kept as held-out data for evaluation.

Dataset	Total Samples	# Observational Samples	# Gene Interventions
[Replogle et al., 2022] K562	162 751	10 691	622
[Replogle et al., 2022] RPE1	162 733	11 485	383

(Kowalczyk et al. [2015]) - making sampling time a potential confounding factor in any analysis of scRNAseq data.

## 4 Benchmarking Setup

**Datasets for causal network inference** Effective GRN inference relies on gene expression datasets of sufficiently large size to infer underlying transcriptional relationships between genes. The size of the MECs inferred by these methods can hypothetically be reduced by using interventional data [Katz et al., 2019]. For our analysis, we make use of gene expression data measured at the resolution of individual cells following a wide range of genetic perturbations. Each perturbation corresponds to the knock down of a specific gene using CRISPRi gene-editing technology [Larson et al., 2013]. This is the largest and best quality dataset of its kind that is publicly available [Peidli et al., 2022], and includes two different biological contexts (cell lines RPE-1 and K562). The dataset is provided in a standardized format that does not require specialized libraries. We have also preprocessed the data so that the expression counts are normalized across batches and perturbations that appear to not have knocked down their target successfully are removed. The goal was to ensure that this benchmark is readily accessible to a broad machine learning audience while requiring no prior domain knowledge of biology beyond what is in this paper. A summary of the resulting two datasets can be found in Table 1. We hold out 20% of the data for evaluation, stratified by intervention target.

**Preprocessing** We incorporated a two-level quality control mechanism for processing our data, considering the perturbations and individual cells separately.

In the perturbation-level control, we identified ‘strong’ perturbations based on three criteria adopted from Replogle et al. [2022]: (1) inducing at least 50 differentially expressed genes with a significance of  $p < 0.05$  according to the Anderson-Darling test after Benjamini-Hochberg correction; (2) being represented in a minimum of 25 cells passing our quality filters; and (3) achieving an on-target knockdown of at least 30%, if measured.

In the individual cell-level control, we checked the effectiveness of each perturbation by contrasting the expression level of the perturbed gene (X) post-perturbation against its baseline level. We established a threshold for expression level at the 10th percentile of gene X in the unperturbed control distribution. We excluded any cell where gene X was perturbed but its expression exceeded this threshold. However, if a perturbed gene’s expression was not measured in the dataset, we did not perform this filtering.

**Network inference model input and output** The benchmarked methods are given either observational data only or both observational and interventional data – depending on the setting – consisting of the expression of each gene in each cell. For interventional data, the target gene in each cell is also given as input. We do not enforce that the methods need to learn a graph on all the variables, and further preprocessing and variables selection is permitted. The only expected output is a list of gene pairs that represent directed edges. No properties of the output network, such as acyclicity, are enforced either.

**Baseline models** We implement a representative set of existing state-of-the-art methods for the task of causal discovery from single-cell observational and mixed perturbational data. For the observational setting, we implement PC (named after the inventors, Peter and Clark; a constraint-based method) [Spirtes et al., 2000], Greedy Equivalence Search (GES; a score-based method) [Chickering, 2002], and NOTEARS variants NOTEARS (Linear), NOTEARS (Linear, L1), NOTEARS (MLP) and

NOTEARS (MLP, L1) [Zheng et al., 2018, 2020], Sortnregress [Reisach et al., 2021] (a marginal variance based method) and GRNBoost [Aibar et al., 2017] (a tree-based GRN inference method). In the interventional setting, we included Greedy Interventional Equivalence Search (GIES, a score-based method and extension to GES) [Hauser and Bühlmann, 2012], the Differentiable Causal Discovery from Interventional Data (DCDI) variants DCDI-G and DCDI-DSF (continuous optimization-based methods) [Brouillard et al., 2020], and DCDI-FG [Lopez et al., 2022]. GES and GIES greedily add and remove edges until a score on the graph is maximized. NOTEARS, DCDI-FG, and DCDI enforce acyclicity via a continuously differentiable constraint, making them suitable for deep learning.

**Benchmark usage** CausalBench has been designed to be easy to setup and use. Adding or testing a new method is also straightforward. A more comprehensive guide can be found in the README of the Github repository (<https://github.com/causalbench/causalbench>) as well as the starter repository of the CausalBench challenge (<https://github.com/causalbench/causalbench-starter/>).

## 5 Evaluation

In CausalBench, unlike standard benchmarks with known or simulated graphs, the true causal graph is unknown due to the complex biological processes involved. This absence of a definitive ground truth presents unique challenges when trying to evidence the superiority of one method over another. We respond to this by developing synergistic metrics with the aim of measuring the accuracy of the output network in representing the underlying complex biological processes. We employ two evaluation types: a biology-driven approximation of ground truth and a quantitative statistical evaluation. The former, though not fully cell-specific, adds an extra validation layer based on known biology. However, we mainly use a new statistical metric for model comparison, which is independent of prior knowledge and data-dependent, and correlates well with relevant downstream applications.

### 5.1 Biological evaluation

The biologically-motivated evaluation in CausalBench is based on biological databases of known putatively causal gene–gene interactions. Using these databases of domain knowledge, we can construct putatively true undirected subnetworks to evaluate the output networks in the understanding that the discovered edges that are not present in those databases are not necessarily false positives. We can then compute metrics such as precision and recall against those constructed networks.

**Biological evaluations metrics** To implement the biologically-motivated evaluation, we extract network data from two widely used open biological databases: CORUM [Giurgiu et al., 2019] and STRING [Von Mering et al., 2005, Snel et al., 2000, Von Mering et al., 2007, Jensen et al., 2009, Mering et al., 2003, Szklarczyk et al., 2010, 2015, 2016, 2019, 2021, Franceschini et al., 2012, 2016]. CORUM is a repository of experimentally characterized protein complexes from mammalian organisms. The complexes are extracted from individual experimental publications, and exclude results from high-throughput experiments. We extract the human protein complexes from the CORUM repository and aggregate them to form a network of genes. STRING is a repository of known and predicted protein-protein interactions. STRING contains both physical (direct) interactions and indirect (functional) interactions that we use to create two evaluation networks from STRING: Protein-protein interactions (network) and protein-protein interactions (physical). Protein-protein interactions (physical) contains only physical interactions, whereas protein-protein interactions (network) contains all types of know and predicted interactions. STRING, and in particular string-network, can contain less reliable links, as the content of the database is pulled from a variety of evidence, such as high-throughput lab experiments, (conserved) co-expression, and text-mining of the literature. Recognizing the importance of considering cell type-specific effects when evaluating gene regulatory network inference methods, we also incorporate cell-type-specific networks for the biological evaluation. For the K562 cell line, we employed data from the Chip-Atlas [Zou et al., 2022] and ENCODE [Davis et al., 2018] databases to build a ChIPSeq networks, restricting the links to those relevant to or recorded in the K562 cell line. However, the RPE1 cell line has not been as comprehensively characterized in existing research. To address this, we utilized networks derived in a similar manner, but from a more extensively studied epithelial cell line, HepG2, given that RPE1 is also an epithelial cell line.

## 5.2 Statistical evaluation

In contrast to the biologically-motivated evaluation, the statistical evaluation in CausalBench is data-driven, cell-specific, and does not rely on prior knowledge. This evaluation method is uniquely designed for single-cell perturbational data and provides a new way to approximate ground-truth gene regulatory interactions, supplementing information found in biological databases. The evaluation uses the interventional data from perturbational scRNA-seq experiments to assess predicted edges in the output networks. Here, we thus closely follow the postulate of Gentzel et al. [2019] that causal methods should be evaluated on empirical data using interventional metrics that correlate with the strength of the underlying relationships.

The main assumption for this evaluation is that if the predicted edge from  $A$  to  $B$  is a true edge denoting a functional interaction between the two genes, then perturbing gene  $A$  should have a statistically significant effect on the distribution  $P^{\sigma(X_A)}(\mathbf{x}_B)$  of values that gene  $B$  takes in the transcription profile, compared to its observational distribution  $P^{\theta}(\mathbf{x}_B)$  (i.e compared to control samples where no gene was perturbed). Conversely, we can test for the predicted absence of gene interactions. We call a gene interaction  $A$  to  $B$  negative if there is no path in the predicted graph from  $A$  to  $B$ . If no interaction exists in the true graph, then there should be no statistically significant change in the distribution of  $B$  when intervening on  $A$ . We thus aim to estimate the false omission rate (FOR) of the predicted graph. The FOR is defined as:

$$\text{FOR} = \frac{\text{False Negatives}}{\text{False Negatives} + \text{True Negatives}}$$

To test the predicted interactions, we propose using the mean Wasserstein distance. For each edge from  $A$  to  $B$ , we compute a Wasserstein distance [Ramdas et al., 2017] between the two empirical distributions of  $P^{\sigma(X_A)}(\mathbf{x}_B)$  and  $P^{\theta}(\mathbf{x}_B)$ . We then return the mean Wasserstein distance of all inferred edges. We call this metric the mean Wasserstein. A higher mean Wasserstein distance should indicate a stronger interventional effect of intervening on the parent. Although the quantitative statistical approach cannot differentiate between causal effects from direct edges or causal paths in the graph, we expect direct relationships to have stronger causal effects [Meinshausen et al., 2016]. Despite this limitation, the quantitative evaluation offers a data-driven, cell-specific, and prior-free metric. It also correlates with the strength of the causal effects, and thus evaluates methods in their ability to recall the strongest perturbational effects, which is a downstream task of high interest. Moreover, it presents a novel approach for estimating ground-truth gene regulatory interactions that is uniquely made possible through the size and interventional nature of single-cell perturbational datasets. Then, we evaluate the predicted negative interactions of the output. To do so, we sample random pairs of genes such that there is no path in the predicted graph between the two. We then perform a two-sided Mann–Whitney U rank test [Mann and Whitney, 1947, Bucchianico, 1999] between samples from  $P^{\sigma(X_A)}(\mathbf{x}_B)$  and  $P^{\theta}(\mathbf{x}_B)$  for all sampled negative pairs using the SciPy package [Virtanen et al., 2020] to test the null hypothesis that the two distributions are equal. A rejected test, with a p-value threshold of 5%, indicates a false negative. The trade-off between maximizing the mean Wasserstein and minimizing the FOR exhibits the ranking nature of this applied task, as opposed to predicting against a fixed binary ground-truth. Contrary to structural metrics, errors in prediction are weighted given their causal importance [Gentzel et al., 2019]. To our knowledge, we are also the first to propose evaluation of the negative predictions.

**Analysis of the proposed quantitative evaluations** We here perform an analysis of the proposed metrics to validate their meaningfulness and to study their properties. We follow a procedure similar to Gentzel et al. [2019]. We create a synthetic dataset using a additive noise model with random Fourier features, reusing code from Lorch et al. [2022]. The training set consists of 500 samples and the test set consists of 1500 observational samples and 30 interventional samples per variable, which makes the test set comparable to the test sets in CausalBench. We then train the Notears (MLP, L1) model with various strengths of sparsity regularization ( $l \in \{0.025, 0.05, 0.1, 0.2, 0.5, 0.75, 1.0\}$ ), repeated five times per value of  $l$ . The results are presented in fig. 2. As can be observed, our proposed statistical metrics highlight the trade-off between recovering and omitting causal relationships, where a stronger regularization value leads to a smaller graph recalling the strongest causal relationship, but omitting many others. At the other end of the spectrum, we can see that at a value of  $l = 0.05$  all causal relationships are recalled as the FOR is 5%, which is equal to the p-value threshold. Lastly,

we can observe that the mean Wasserstein is well correlated with a structural metric such as SHD, but that it gives a better ordering of the models that is weighted in terms of strength of the predicted causal relationship. As such, our proposed statistical metrics are well suited for applied tasks and offer a meaningful tool for model comparison and selection in practice.

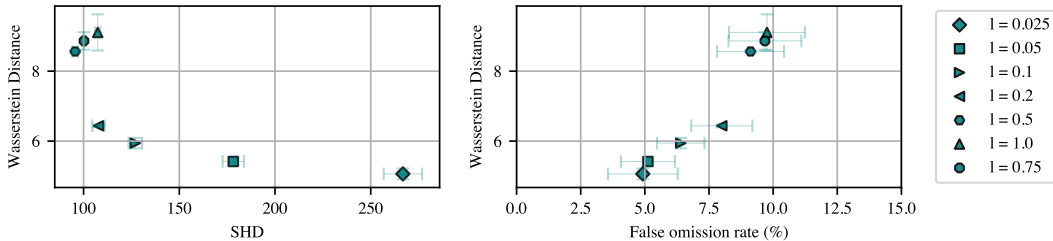


Figure 2: Plots showing the characteristics of the proposed statistical evaluations, here validated on synthetic data. A NOTEARS (MLP, L1) model is run with different regularization values. Each setting is run five times, with the mean and standard deviation score plotted across the five runs for each setting.

### 5.3 Characteristics of the optimal method

For actual applicability to this real-world setting, the optimal method should exhibit properties that go beyond best relative performance on the metrics presented previously. First, to uncover interactions among all encoding genes, the optimal graph inference method should computationally scale to graphs with a large number of nodes (in the thousands). Furthermore, the method performance should increase as more samples and more targeted genes are given as input. This ensures that the method is future-proof as we expect larger datasets that target almost all possible genes to become ubiquitous in the near future. The scale of the datasets used here allows us to test for these scaling properties in our benchmark by making the creation of settings with varying fractions of data or of number of interventions easy and principled.

## 6 Benchmarking Results

### 6.1 Network inference

We here summarize the experimental results of our baselines in both observational and interventional settings, on the statistical evaluations and the biologically-motivated evaluations. All results are obtained by training on the full dataset three times with different random seeds.

**Trade-off between precision and recall** We highlight the trade-off between recall and precision. Indeed, we expect methods to optimize for these two goals, as we want to obtain a high precision while maximizing the percentage of discovered interactions. On both the biological and statistical evaluation, we observe this trade-off, as most of the baseline methods tend to gravitate toward one extreme or the other. That is, they either prioritize precision at the cost of uncovering fewer interactions, or they uncover a larger number of interactions but with less precision. GRNBoost is the only method with a high recall, but this comes with low precision. Most of the other baselines have similar recall and varying precision. Results are summarized in fig. 3. As can be observed, there is no major difference in performance between observational and interventional methods.

**Causal models that leverage interventional information do not outperform the others** We observe that, contrary to what would be theoretically expected, interventional methods do not outperform observational methods, even though they are trained on more informative data. For example, on both datasets, GIES does not outperform its observational counterpart GES. Also, simple non-causal methods such as GRNBoost and Sortnregress perform highly. GRNBoost performance is mainly driven by its capacity to recall most causal interactions, at the expense of its precision. Sortnregress performance shows that even the varsortability [Reisach et al., 2021] of the two datasets is underexploited by most methods. Lastly, DCDI-G shows high mean Wasserstein,



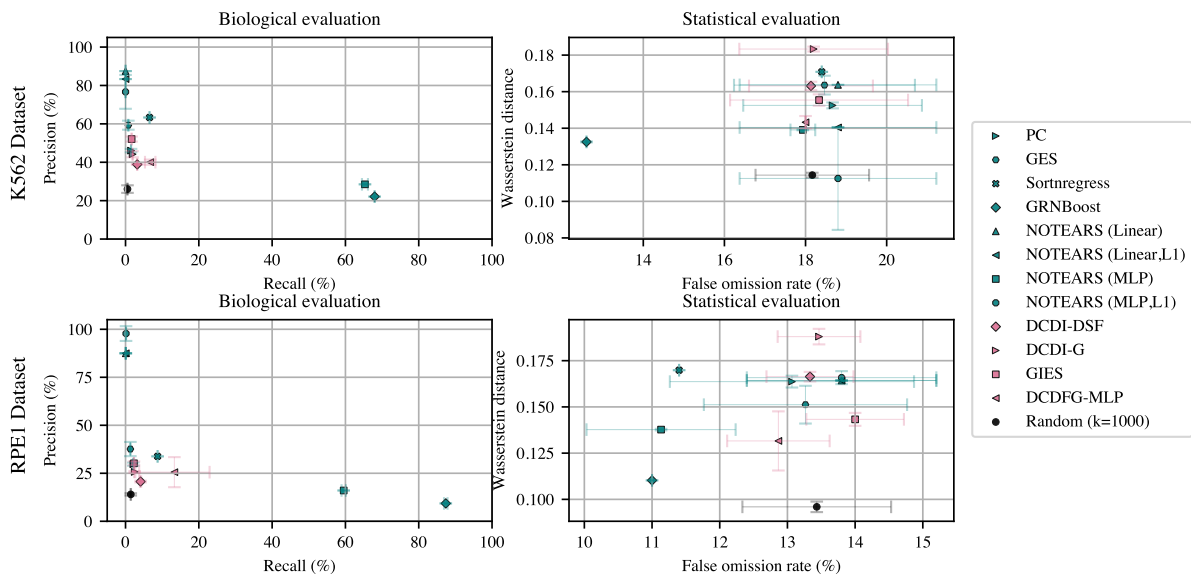


Figure 3: Performance comparison in terms of Precision (in %; y-axis) and Recall (in %; x-axis) in correctly identifying edges substantiated by biological interaction databases (left panels); and our own statistical evaluation using interventional information in terms of Wasserstein distance and FOR (right panels). Performance is compared across 8 different methods using observational data (green markers), 4 different methods using interventional data (pink markers), and 1 random baseline (black markers) in K562 (top panels) and RPE1 (bottom panels) cell lines. For each method, we show the mean and standard deviation from three independent runs. Complete and detailed results can be found in appendix B.

which demonstrates some capacity to leverage the interventional data, but it omits a large number of interactions given it cannot infer the graph on all variables. This highlights an opportunity for further method development for causal graph inference in order to be able to fully leverage interventional data. Early results in this direction were made possible using CausalBench to organize a community machine learning challenge. To summarize the performance of the baselines, we propose a simple and unbiased way to compute a ranked scoreboard that takes into account the Wasserstein score and FOR. The detailed ranking can be found in appendix D, and a summary is given in table 2.

## 6.2 No model fulfills all the characteristics of an optimal method for this task

**Most methods do not scale to the full graph.** Unfortunately, all tested methods, with the exception of NOTEARS, GRNBoost, DCDFG and Sortnregress, do not computationally scale to graphs of the size typically encountered in transcriptome-wide GRN inference. Nonetheless, to enable a meaningful comparison, we partitioned the variables into smaller subsets where necessary and ran the methods on each subset independently, with the final output network being the union of the subnetworks. The proposed approach breaks the no-latent-confounder assumption that some methods may make, and it also does not fully leverage the information potentially available within the data. Methods that do scale to the full graph in a single optimization loop should therefore perform better.

**Performance as a function of sample size.** We additionally studied the effect of sample size on the performance of the evaluated state-of-the-art models. We randomly subset the data at different fractions and report the mean Wasserstein distance as explained in the quantitative evaluations part of Section 5.2 and shown in Figure 5. In the observational setting, the sample size does not seem to have a significant effect on performance for most methods, indeed having a slightly negative effect for some methods. In the interventional setting, a positive impact is observable for a larger sample size, especially for the methods that rely on deep networks and gradient-based learning such as DCDI, whereas GIES seems to suffer in a large sample setting.

Table 2: Table summarizing the characteristics of the test baselines as laid out in section 5.3 and analysed in section 6.2, as well as two per dataset rankings. Graph scaling refers to the ability to infer on the complete set of genes. A method is deemed to have successfully achieved sample scaling and intervention scaling if its performance improves by at least 10% on both datasets. This comparison is made between settings where only a subset, specifically 25% of samples or perturbations, is used and settings where 100% of them are utilized. As such, no baseline fulfills all the criteria. Details on the ranking can be found in appendix D.

Model	Graph scaling	Sample scaling	Intervention scaling	Ranking K562	Ranking RPE1
PC	×	×	–	GRNBoost	Sortnregress
GES	×	×	–	DCDI-G	GRNBoost
GIES	×	×	×	Sortnregress	DCDI-G
NOTEARS	✓	×	–	DCDI-DSF	NOTEARS (MLP)
DCDI-G	×	✓	×	GES	PC
DCDI-DSF	×	×	×	NOTEARS (Linear)	DCDI-DSF
DCDI-FG	✓	×	×	GIES	NOTEARS (MLP,L1)
GRNBoost	✓	×	–	PC	NOTEARS (Linear)
Sortnregress	✓	×	–	NOTEARS (MLP)	NOTEARS (Linear,L1)
				DCDFG-MLP	DCDFG-MLP
				NOTEARS (Linear,L1)	GES
				NOTEARS (MLP,L1)	GIES

**Performance by the fraction of perturbations.** Beyond the size of the training set, we also studied the partial interventional setting – where only a subset of the possible genes to perturb are experimentally targeted. We adapt the fraction of randomly targeted genes from 5% (low ratio of interventions) to 100% (fully interventional). We randomly subset the genes at different fractions, using three different random seeds for each method, and report the mean Wasserstein distance as a measure of quantitative evaluation. We would expect a larger fraction of intervened genes to lead to higher performance, as this should facilitate the identification of the true causal graph. We indeed observe a better performance for DCDI on K562 as we increase the fraction of intervened genes. For GIES, we again observe a negative effect of having more data on RPE1.

### 6.3 Compute resources

All methods were given the same computational resources, which consists of 20 CPU’s with 32GB of memory each. We additionally assign a GPU for the DCDI and DCDFG methods. The hyperparameters of each method, such as partition sizes, are chosen such that the running time remains below 30 hours. Partition sizes for each model can be found in appendix C.

### 6.4 Limitations.

Openly available benchmarks for causal models for large-scale single-cell data could potentially accelerate the development of new and effective approaches for uncovering gene regulatory relationships. However, some limitations to this approach remain: firstly, the biological networks used for evaluation do not fully capture ground-truth GRNs, and the reported connection are often biased towards better-studied systems and pathways [Gillis et al., 2014]. True ground-truth validation would require prospective and exhaustive interventional wet-lab experiments. However, at present, experiments at the scale necessary to exhaustively map gene–gene interactions across the genome are cost prohibitive for all possible edges. Beyond limitations in data sources used, there are limitations with some of the assumptions in the utilized state-of-the-art models. For instance, feedback loops between genes are a well-known phenomenon in gene regulation [Carthew, 2006, Levine and Davidson, 2005] that unfortunately cannot be represented by most existing causal network inference methods at present. While many causal discovery methods assume causal sufficiency, which posits that all common causes of any pair of variables are observed, it is important to note that this assumption may not hold true in the datasets included in CausalBench. Lastly, the assumption of linearity of interaction may not hold for gene-gene interactions. We acknowledge these limitations and encourage ongoing research to address them.

## 7 Conclusion

We introduced CausalBench – a comprehensive open benchmark for evaluating causal discovery algorithms on real-world interventional data, using two large-scale CRISPR-based interventional scRNA-seq datasets. CausalBench introduces a set of biologically meaningful performance metrics to quantitatively compare graphs that are proposed by causal inference methods using novel statistical evaluations, and validated them according to existing biological knowledge bases. CausalBench was designed to streamline the evaluation of causal discovery methods on real-world interventional data by standardizing non-model-related components of the evaluation process, thereby allowing researchers to focus on advancing causal network discovery methods. With more than 200 000 interventional samples, CausalBench is built on one of the largest open real-world interventional datasets [Replogle et al., 2022], providing the causal machine learning community with unprecedented access to large-scale interventional data for developing and evaluating causal discovery methods. Our results highlight many challenges faced by existing models applied to this challenging domain, such as poor scalability and inadequate utilization of the interventional data. Major strides in this direction have already been made, as evidenced by a recent machine learning community challenge that successfully utilized CausalBench (see <https://www.gsk.ai/causalbench-challenge/> for details).

## Acknowledgements and disclosure

The authors thank Prof. Nicolai Meinshausen for feedback and comments on the statistical evaluations and on the manuscript. We also thank Siobhan Sanford and Djordje Miladinovic for comments and edits on the manuscript. MC, YR, AM and PS are employees and shareholders of GSK plc.

## References

- S. Aibar, C. B. González-Blas, T. Moerman, V. A. Huynh-Thu, H. Imrichova, G. Hulselmans, F. Rambow, J.-C. Marine, P. Geurts, J. Aerts, et al. Scenic: single-cell regulatory network inference and clustering. *Nature methods*, 14(11):1083–1086, 2017.
- K. Akers and T. Murali. Gene regulatory network inference in single-cell biology. *Current Opinion in Systems Biology*, 26:87–97, 2021.
- A.-L. Barabási and R. Albert. Emergence of scaling in random networks. *science*, 286(5439):509–512, 1999.
- N. Baum-Snow and F. Ferreira. Causal inference in urban and regional economics. In *Handbook of regional and urban economics*, volume 5, pages 3–68. Elsevier, 2015.
- P. Brouillard, S. Lachapelle, A. Lacoste, S. Lacoste-Julien, and A. Drouin. Differentiable causal discovery from interventional data. *Advances in Neural Information Processing Systems*, 33:21865–21877, 2020.
- A. D. Buccianico. Combinatorics, computer algebra, and the Wilcoxon-Mann-Whitney test”. *Journal of Statistical Planning and Inference*, 79:349–364, 1999.
- R. W. Carthew. Gene regulation by micrnas. *Current opinion in genetics & development*, 16(2):203–208, 2006.
- L. E. Chai, S. K. Loh, S. T. Low, M. S. Mohamad, S. Deris, and Z. Zakaria. A review on the computational approaches for gene regulatory network construction. *Computers in biology and medicine*, 48:55–65, 2014.
- D. M. Chickering. Optimal structure identification with greedy search. *Journal of machine learning research*, 3(Nov):507–554, 2002.
- P. Datlinger, A. F. Rendeiro, C. Schmidl, T. Krausgruber, P. Traxler, J. Klughammer, L. C. Schuster, A. Kuchler, D. Alpar, and C. Bock. Pooled crispr screening with single-cell transcriptome readout. *Nature methods*, 14(3):297–301, 2017.

- P. Datlinger, A. F. Rendeiro, T. Boenke, M. Senekowitsch, T. Krausgruber, D. Barreca, and C. Bock. Ultra-high-throughput single-cell rna sequencing and perturbation screening with combinatorial fluidic indexing. *Nature methods*, 18(6):635–642, 2021.
- C. A. Davis, B. C. Hitz, C. A. Sloan, E. T. Chan, J. M. Davidson, I. Gabdank, J. A. Hilton, K. Jain, U. K. Baymuradov, A. K. Narayanan, et al. The encyclopedia of dna elements (encode): data portal update. *Nucleic acids research*, 46(D1):D794–D801, 2018.
- J. Deng, W. Dong, R. Socher, L.-J. Li, K. Li, and L. Fei-Fei. Imagenet: A large-scale hierarchical image database. In *2009 IEEE conference on computer vision and pattern recognition*, pages 248–255. Ieee, 2009.
- P. Dibaeinia and S. Sinha. Sergio: a single-cell expression simulator guided by gene regulatory networks. *Cell systems*, 11(3):252–271, 2020.
- A. Dixit, O. Parnas, B. Li, J. Chen, C. P. Fulco, L. Jerby-Arnon, N. D. Marjanovic, D. Dionne, T. Burks, R. Raychowdhury, et al. Perturb-seq: dissecting molecular circuits with scalable single-cell rna profiling of pooled genetic screens. *cell*, 167(7):1853–1866, 2016.
- P. Erdős, A. Rényi, et al. On the evolution of random graphs. *Publ. Math. Inst. Hung. Acad. Sci*, 5(1): 17–60, 1960.
- R. E. Farmer, D. Kounali, A. S. Walker, J. Savović, A. Richards, M. T. May, and D. Ford. Application of causal inference methods in the analyses of randomised controlled trials: a systematic review. *Trials*, 19:1–14, 2018.
- A. Franceschini, D. Szklarczyk, S. Frankild, M. Kuhn, M. Simonovic, A. Roth, J. Lin, P. Minguez, P. Bork, C. Von Mering, et al. String v9. 1: protein-protein interaction networks, with increased coverage and integration. *Nucleic acids research*, 41(D1):D808–D815, 2012.
- A. Franceschini, J. Lin, C. von Mering, and L. J. Jensen. Svd-phy: improved prediction of protein functional associations through singular value decomposition of phylogenetic profiles. *Bioinformatics*, 32(7):1085–1087, 2016.
- N. Friedman, M. Linial, I. Nachman, and D. Pe’er. Using bayesian networks to analyze expression data. *Journal of computational biology*, 7(3-4):601–620, 2000.
- A. Gentzel, D. Garant, and D. Jensen. The case for evaluating causal models using interventional measures and empirical data. *Advances in Neural Information Processing Systems*, 32, 2019.
- J. Gillis, S. Ballouz, and P. Pavlidis. Bias tradeoffs in the creation and analysis of protein–protein interaction networks. *Journal of proteomics*, 100:44–54, 2014.
- M. Giurgiu, J. Reinhard, B. Brauner, I. Dunger-Kaltenbach, G. Fobo, G. Frishman, C. Montrone, and A. Ruepp. Corum: the comprehensive resource of mammalian protein complexes—2019. *Nucleic acids research*, 47(D1):D559–D563, 2019.
- A. Hauser and P. Bühlmann. Characterization and greedy learning of interventional markov equivalence classes of directed acyclic graphs. *The Journal of Machine Learning Research*, 13(1): 2409–2464, 2012.
- X. Hu, Y. Hu, F. Wu, R. W. T. Leung, and J. Qin. Integration of single-cell multi-omics for gene regulatory network inference. *Computational and Structural Biotechnology Journal*, 18:1925–1938, 2020.
- B. Huang, K. Zhang, Y. Lin, B. Schölkopf, and C. Glymour. Generalized score functions for causal discovery. In *Proceedings of the 24th ACM SIGKDD international conference on knowledge discovery & data mining*, pages 1551–1560, 2018.
- V. A. Huynh-Thu, A. Irrthum, L. Wehenkel, and P. Geurts. Inferring regulatory networks from expression data using tree-based methods. *PloS one*, 5(9):e12776, 2010.
- L. J. Jensen, M. Kuhn, M. Stark, S. Chaffron, C. Creevey, J. Muller, T. Doerks, P. Julien, A. Roth, M. Simonovic, et al. String 8—a global view on proteins and their functional interactions in 630 organisms. *Nucleic acids research*, 37(suppl\_1):D412–D416, 2009.

- M. Joffe, M. Gambhir, M. Chadeau-Hyam, and P. Vineis. Causal diagrams in systems epidemiology. *Emerging themes in epidemiology*, 9(1):1–18, 2012.
- K. Kamimoto, C. M. Hoffmann, and S. A. Morris. Celloracle: Dissecting cell identity via network inference and in silico gene perturbation. *BioRxiv*, 2020.
- D. Katz, K. Shanmugam, C. Squires, and C. Uhler. Size of interventional markov equivalence classes in random dag models. In *The 22nd International Conference on Artificial Intelligence and Statistics*, pages 3234–3243. PMLR, 2019.
- N. R. Ke, O. Bilaniuk, A. Goyal, S. Bauer, H. Larochelle, B. Schölkopf, M. C. Mozer, C. Pal, and Y. Bengio. Learning neural causal models from unknown interventions. *arXiv preprint arXiv:1910.01075*, 2019.
- M. S. Kowalczyk, I. Tirosh, D. Heckl, T. N. Rao, A. Dixit, B. J. Haas, R. K. Schneider, A. J. Wagers, B. L. Ebert, and A. Regev. Single-cell rna-seq reveals changes in cell cycle and differentiation programs upon aging of hematopoietic stem cells. *Genome research*, 25(12):1860–1872, 2015.
- M. H. Larson, L. A. Gilbert, X. Wang, W. A. Lim, J. S. Weissman, and L. S. Qi. Crispr interference (crispr) for sequence-specific control of gene expression. *Nature protocols*, 8(11):2180–2196, 2013.
- M. Levine and E. H. Davidson. Gene regulatory networks for development. *Proceedings of the National Academy of Sciences*, 102(14):4936–4942, 2005.
- R. Lopez, J.-C. Hütter, J. K. Pritchard, and A. Regev. Large-scale differentiable causal discovery of factor graphs. *arXiv preprint arXiv:2206.07824*, 2022.
- L. Lorch, S. Sussex, J. Rothfuss, A. Krause, and B. Schölkopf. Amortized inference for causal structure learning. *arXiv preprint arXiv:2205.12934*, 2022.
- H. B. Mann and D. R. Whitney. On a test of whether one of two random variables is stochastically larger than the other. *The annals of mathematical statistics*, pages 50–60, 1947.
- A. Mehrjou, A. Soleymani, A. Jesson, P. Notin, Y. Gal, S. Bauer, and P. Schwab. GeneDisco: A Benchmark for Experimental Design in Drug Discovery. In *International Conference on Learning Representations*, 2022.
- N. Meinshausen, A. Hauser, J. M. Mooij, J. Peters, P. Versteeg, and P. Bühlmann. Methods for causal inference from gene perturbation experiments and validation. *Proceedings of the National Academy of Sciences*, 113(27):7361–7368, 2016.
- C. v. Mering, M. Huynen, D. Jaeggi, S. Schmidt, P. Bork, and B. Snel. String: a database of predicted functional associations between proteins. *Nucleic acids research*, 31(1):258–261, 2003.
- B. Neal, C.-W. Huang, and S. Raghupathi. Realcause: Realistic causal inference benchmarking. *arXiv preprint arXiv:2011.15007*, 2020.
- M. R. Nelson, H. Tipney, J. L. Painter, J. Shen, P. Nicoletti, Y. Shen, A. Floratos, P. C. Sham, M. J. Li, J. Wang, et al. The support of human genetic evidence for approved drug indications. *Nature genetics*, 47(8):856–860, 2015.
- H. Parikh, C. Varjao, L. Xu, and E. Tchetgen. Validating causal inference methods. In *International Conference on Machine Learning*, pages 17346–17358. PMLR, 2022.
- J. Pearl. *Causality*. Cambridge university press, 2009.
- S. Peidli, T. D. Green, C. Shen, T. Gross, J. Min, S. Garda, B. Yuan, L. J. Schumacher, J. P. Taylor-King, D. S. Marks, et al. scperturb: Harmonized single-cell perturbation data. *bioRxiv*, pages 2022–08, 2022.
- J. Peters and P. Bühlmann. Structural intervention distance for evaluating causal graphs. *Neural computation*, 27(3):771–799, 2015.

- J. Peters, D. Janzing, and B. Schölkopf. *Elements of causal inference: foundations and learning algorithms*. The MIT Press, 2017.
- A. Pratapa, A. P. Jaliyal, J. N. Law, A. Bharadwaj, and T. Murali. Benchmarking algorithms for gene regulatory network inference from single-cell transcriptomic data. *Nature methods*, 17(2):147–154, 2020.
- A. Ramdas, N. García Trillos, and M. Cuturi. On wasserstein two-sample testing and related families of nonparametric tests. *Entropy*, 19(2):47, 2017.
- A. Reisach, C. Seiler, and S. Weichwald. Beware of the simulated dag! causal discovery benchmarks may be easy to game. *Advances in Neural Information Processing Systems*, 34:27772–27784, 2021.
- J. M. Replogle, R. A. Saunders, A. N. Pogson, J. A. Hussmann, A. Lenail, A. Guna, L. Mascibroda, E. J. Wagner, K. Adelman, G. Lithwick-Yanai, et al. Mapping information-rich genotype-phenotype landscapes with genome-scale perturb-seq. *Cell*, 2022.
- N. Scherrer, O. Bilaniuk, Y. Annadani, A. Goyal, P. Schwab, B. Schölkopf, M. C. Mozer, Y. Bengio, S. Bauer, and N. R. Ke. Learning neural causal models with active interventions. *arXiv preprint arXiv:2109.02429*, 2021.
- B. Schölkopf, F. Locatello, S. Bauer, N. R. Ke, N. Kalchbrenner, A. Goyal, and Y. Bengio. Toward causal representation learning. *Proceedings of the IEEE*, 109(5):612–634, 2021.
- E. Shifrut, J. Carnevale, V. Tobin, T. L. Roth, J. M. Woo, C. T. Bui, P. J. Li, M. E. Diolaiti, A. Ashworth, and A. Marson. Genome-wide crispr screens in primary human t cells reveal key regulators of immune function. *Cell*, 175(7):1958–1971, 2018.
- Y. Shimoni, C. Yanover, E. Karavani, and Y. Goldschmidt. Benchmarking framework for performance-evaluation of causal inference analysis. *arXiv preprint arXiv:1802.05046*, 2018.
- J. P. Simmons, L. D. Nelson, and U. Simonsohn. False-positive psychology: Undisclosed flexibility in data collection and analysis allows presenting anything as significant. *Psychological science*, 22(11):1359–1366, 2011.
- B. Snel, G. Lehmann, P. Bork, and M. A. Huynen. String: a web-server to retrieve and display the repeatedly occurring neighbourhood of a gene. *Nucleic acids research*, 28(18):3442–3444, 2000.
- P. Spirtes, C. N. Glymour, R. Scheines, and D. Heckerman. *Causation, prediction, and search*. MIT press, 2000.
- D. Szklarczyk, A. Franceschini, M. Kuhn, M. Simonovic, A. Roth, P. Minguéz, T. Doerks, M. Stark, J. Muller, P. Bork, et al. The string database in 2011: functional interaction networks of proteins, globally integrated and scored. *Nucleic acids research*, 39(suppl\_1):D561–D568, 2010.
- D. Szklarczyk, A. Franceschini, S. Wyder, K. Forslund, D. Heller, J. Huerta-Cepas, M. Simonovic, A. Roth, A. Santos, K. P. Tsafou, et al. String v10: protein–protein interaction networks, integrated over the tree of life. *Nucleic acids research*, 43(D1):D447–D452, 2015.
- D. Szklarczyk, J. H. Morris, H. Cook, M. Kuhn, S. Wyder, M. Simonovic, A. Santos, N. T. Doncheva, A. Roth, P. Bork, et al. The string database in 2017: quality-controlled protein–protein association networks, made broadly accessible. *Nucleic acids research*, page gkw937, 2016.
- D. Szklarczyk, A. L. Gable, D. Lyon, A. Junge, S. Wyder, J. Huerta-Cepas, M. Simonovic, N. T. Doncheva, J. H. Morris, P. Bork, et al. String v11: protein–protein association networks with increased coverage, supporting functional discovery in genome-wide experimental datasets. *Nucleic acids research*, 47(D1):D607–D613, 2019.
- D. Szklarczyk, A. L. Gable, K. C. Nastou, D. Lyon, R. Kirsch, S. Pyysalo, N. T. Doncheva, M. Legeay, T. Fang, P. Bork, et al. The string database in 2021: customizable protein–protein networks, and functional characterization of user-uploaded gene/measurement sets. *Nucleic acids research*, 49(D1):D605–D612, 2021.

- S. Tracy, G.-C. Yuan, and R. Dries. Rescue: imputing dropout events in single-cell rna-sequencing data. *BMC bioinformatics*, 20(1):1–11, 2019.
- P. Virtanen, R. Gommers, T. E. Oliphant, M. Haberland, T. Reddy, D. Cournapeau, E. Burovski, P. Peterson, W. Weckesser, J. Bright, S. J. van der Walt, M. Brett, J. Wilson, K. J. Millman, N. Mayorov, A. R. J. Nelson, E. Jones, R. Kern, E. Larson, C. J. Carey, Í. Polat, Y. Feng, E. W. Moore, J. VanderPlas, D. Laxalde, J. Perktold, R. Cimrman, I. Henriksen, E. A. Quintero, C. R. Harris, A. M. Archibald, A. H. Ribeiro, F. Pedregosa, P. van Mulbregt, and SciPy 1.0 Contributors. SciPy 1.0: Fundamental Algorithms for Scientific Computing in Python. *Nature Methods*, 17: 261–272, 2020. doi: 10.1038/s41592-019-0686-2.
- C. Von Mering, L. J. Jensen, B. Snel, S. D. Hooper, M. Krupp, M. Foglierini, N. Jouffre, M. A. Huynen, and P. Bork. String: known and predicted protein–protein associations, integrated and transferred across organisms. *Nucleic acids research*, 33(suppl\_1):D433–D437, 2005.
- C. Von Mering, L. J. Jensen, M. Kuhn, S. Chaffron, T. Doerks, B. Krüger, B. Snel, and P. Bork. String 7—recent developments in the integration and prediction of protein interactions. *Nucleic acids research*, 35(suppl\_1):D358–D362, 2007.
- Y. Wang, L. Solus, K. Yang, and C. Uhler. Permutation-based causal inference algorithms with interventions. *Advances in Neural Information Processing Systems*, 30, 2017.
- J. Yu, V. A. Smith, P. P. Wang, A. J. Hartemink, and E. D. Jarvis. Advances to bayesian network inference for generating causal networks from observational biological data. *Bioinformatics*, 20(18):3594–3603, 2004.
- X. Zheng, B. Aragam, P. Ravikumar, and E. P. Xing. DAGs with NO TEARS: Continuous Optimization for Structure Learning. In *Advances in Neural Information Processing Systems*, 2018.
- X. Zheng, C. Dan, B. Aragam, P. Ravikumar, and E. P. Xing. Learning sparse nonparametric DAGs. In *International Conference on Artificial Intelligence and Statistics*, 2020.
- Z. Zou, T. Ohta, F. Miura, and S. Oki. Chip-atlas 2021 update: a data-mining suite for exploring epigenomic landscapes by fully integrating chip-seq, atac-seq and bisulfite-seq data. *Nucleic Acids Research*, page 1, 2022.

## A Baselines descriptions

### A.0.1 PC

is one of the most widely used methods in causal inference from observational data that assumes there are no confounders and calculates conditional independence to give asymptotically correct results. It outputs the equivalence class of graphs that conform with the results of the conditional independence tests.

### A.0.2 Greedy Equivalence Search (GES)

implements a two-phase procedure (Forward and Backward phases that adds and removes edges from the graph) to calculate a score to choose within an equivalence class. While GES leverages only observational data, its extension, Greedy Interventional Equivalence Search (GIES), enhances GES by adding a turning phase to allow for the inclusion of interventional data.

### A.0.3 NOTEARS

formulates the DAG inference problem as a continuous optimization over real-valued matrices that avoids the combinatorial search over acyclic graphs. This is achieved by constructing a smooth function with computable derivatives over the adjacent matrices that vanishes only when the associated graph is acyclic. Various versions of NOTEARS refer to which function approximator is employed (either a MLP or Linear) or which regularity term is added to the loss function (e.g. L1 for the sparsity constraint.)

#### A.0.4 Differentiable Causal Discovery from Interventional Data (DCDI)

[Brouillard et al., 2020] leverages various types of interventions (perfect, imperfect, unknown), and uses a neural network model to capture conditional densities. DCDI encodes the DAG using a binary adjacency matrix. The intervention matrix is also modeled as a binary mask that determines which nodes are the target of intervention. A likelihood-based differentiable objective function is formed by using this parameterization, and subsequently maximized by gradient-based methods to infer the underlying DAG. DCDI-G assumes Gaussian conditional distributions while DCDI-DSF lifts this assumption by using normalizing flows to capture flexible distributions.

#### A.0.5 GRNBoost

[Aibar et al., 2017] is a GRN specific Gradient Boosting tree method, where for every gene, candidate parent gene are ranked based on their predictive power toward the expression profile of the downstream gene. As such, it acts as a feature selection method toward learning the graph. GRNBoost was identified as one of the best performing GRN method in previous observational data based benchmarks [Pratapa et al., 2020].

#### A.0.6 Random (k)

is the simplest baseline which outputs a graph from which  $k$  nodes are selected at uniformly random without replacement. In the experiments, we tested  $k = 100, 1000, \text{ and } 10000$ .

### B Additional results

We here recapitulate more detailed and extensive results of our analysis of stat-of-the-art method using Causalbench. Figure 4 shows the same plot as in the main text but with single run as individual points. Table 4 and table 3 show the precision and recall scores for the biological evaluation for each database. Figure 5 shows the effect of varying the dataset or intervention set size for each method.

Table 3: Performance results on RPE-1 Dataset for the biological evaluation, for each evidence type. Pooled correspond to pooling all the extracted databases into one network for evaluation.

Model	Precision					Recall				
	Pooled	CORUM	PPI (N)	PPI (P)	CHIP	Pooled	CORUM	PPI (N)	PPI (P)	CHIP
GES	0.38±0.04	0.02±0.01	0.37±0.04	0.11±0.02	0.00±0.00	0.01±0.00	0.02±0.00	0.02±0.00	0.02±0.00	0.00±0.00
GRNBoost	0.09±0.00	0.00±0.00	0.08±0.00	0.02±0.00	0.01±0.00	0.87±0.00	0.95±0.01	0.88±0.00	0.89±0.00	0.65±0.01
NOTEARS (Linear)	0.88±0.00	0.12±0.00	0.88±0.00	0.38±0.00	0.00±0.00	0.00±0.00	0.00±0.00	0.00±0.00	0.00±0.00	0.00±0.00
NOTEARS (Linear,L1)	0.88±0.00	0.12±0.00	0.88±0.00	0.38±0.00	0.00±0.00	0.00±0.00	0.00±0.00	0.00±0.00	0.00±0.00	0.00±0.00
NOTEARS (MLP)	0.16±0.00	0.01±0.00	0.14±0.00	0.03±0.00	0.01±0.00	0.60±0.01	0.80±0.01	0.61±0.01	0.61±0.01	0.25±0.00
NOTEARS (MLP,L1)	0.98±0.04	0.15±0.01	0.98±0.04	0.59±0.05	0.00±0.00	0.00±0.00	0.00±0.00	0.00±0.00	0.00±0.00	0.00±0.00
PC	0.30±0.01	0.02±0.00	0.28±0.01	0.08±0.01	0.01±0.00	0.02±0.00	0.03±0.00	0.02±0.00	0.03±0.00	0.00±0.00
Sortnregress	0.34±0.00	0.02±0.00	0.32±0.00	0.09±0.00	0.02±0.00	0.09±0.00	0.11±0.00	0.10±0.00	0.11±0.00	0.02±0.00
GIES	0.30±0.01	0.02±0.01	0.29±0.01	0.08±0.01	0.01±0.00	0.02±0.00	0.03±0.01	0.03±0.00	0.03±0.00	0.00±0.00
DCDFG-MLP	0.26±0.08	0.02±0.01	0.23±0.08	0.05±0.01	0.04±0.01	0.13±0.10	0.15±0.09	0.13±0.10	0.13±0.10	0.12±0.09
DCDI-DSF	0.21±0.00	0.01±0.00	0.20±0.00	0.06±0.00	0.01±0.00	0.04±0.00	0.05±0.00	0.05±0.00	0.05±0.00	0.01±0.00
DCDI-G	0.26±0.00	0.02±0.00	0.25±0.00	0.07±0.00	0.01±0.00	0.03±0.00	0.04±0.01	0.03±0.00	0.04±0.00	0.00±0.00
Random (k=1000)	0.14±0.01	0.01±0.00	0.12±0.01	0.03±0.00	0.01±0.01	0.01±0.00	0.01±0.00	0.01±0.00	0.01±0.00	0.01±0.00

### C Partition sizes

We here recapitulate the partition sizes used to be able to run each method in Table 5.

### D Model ranking

We here present a simple unbiased way of ranking the different models based on the mean Wasserstein distance and the FOR. We separate the rankings per cell type. First, we create a preliminary ranking for each evaluation metrics. We first rank by the mean score across the different seeds. Then, we assign the same rank to all models having overlapping confidence interval, starting from the bottom of the ranking. Finally, for each model, we take their average rank across the evaluation specific



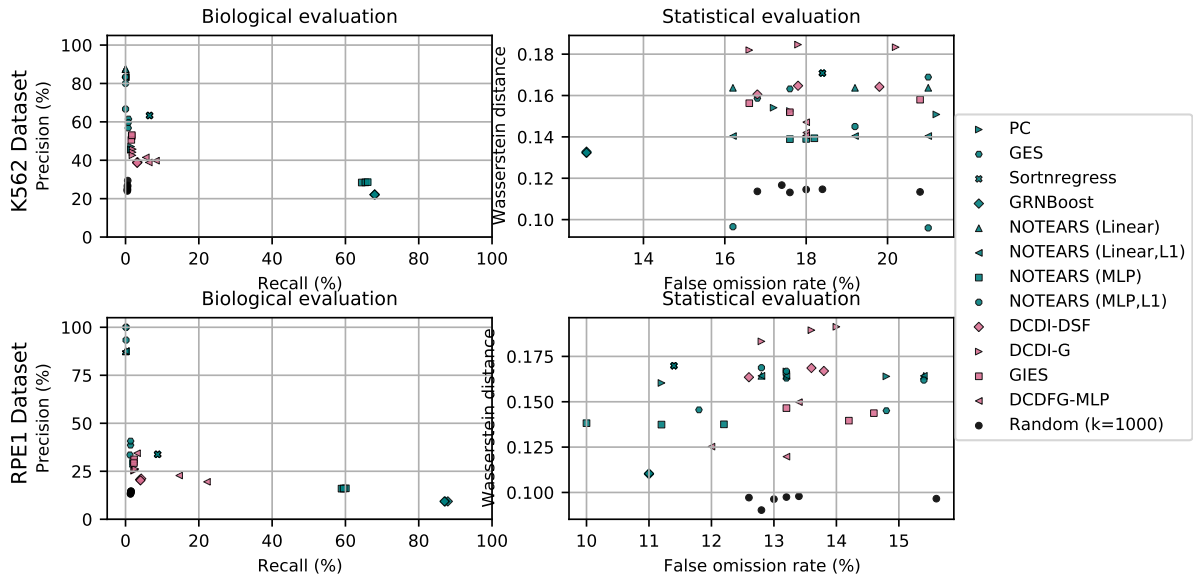


Figure 4: Performance comparison in terms of Precision (in %; y-axis) and Recall (in %; x-axis) in correctly identifying edges substantiated by biological interaction databases (left panels); and our own statistical evaluation using interventional information in terms of Wasserstein distance and FOR (right panels). Performance is compared across 8 different methods using observational data (green markers), 4 different methods using interventional data (pink markers), and 1 random baseline (black markers) in K562 (top panels) and RPE1 (bottom panels) cell lines. For each method, we show the score of three independent runs.

Table 4: Performance results on K562 Dataset for the biological evaluation, for each evidence type. Pooled correspond to pooling all the extracted databases into one network for evaluation.

Model	Precision					Recall				
	Pooled	CORUM	PPI (N)	PPI (P)	CHIP	Pooled	CORUM	PPI (N)	PPI (P)	CHIP
GES	0.59±0.02	0.18±0.01	0.59±0.02	0.26±0.01	0.00±0.00	0.01±0.00	0.03±0.00	0.01±0.00	0.01±0.00	0.00±0.00
GRNBoost	0.22±0.00	0.02±0.00	0.21±0.00	0.07±0.00	0.01±0.00	0.68±0.00	0.81±0.01	0.69±0.00	0.71±0.00	0.32±0.00
NOTEARS (Linear)	0.88±0.00	0.50±0.00	0.88±0.00	0.50±0.00	0.00±0.00	0.00±0.00	0.00±0.00	0.00±0.00	0.00±0.00	0.00±0.00
NOTEARS (Linear,L1)	0.83±0.00	0.50±0.00	0.83±0.00	0.50±0.00	0.00±0.00	0.00±0.00	0.00±0.00	0.00±0.00	0.00±0.00	0.00±0.00
NOTEARS (MLP)	0.29±0.00	0.02±0.00	0.27±0.00	0.08±0.00	0.01±0.00	0.65±0.01	0.53±0.01	0.66±0.01	0.62±0.01	0.27±0.02
NOTEARS (MLP,L1)	0.77±0.09	0.06±0.10	0.77±0.09	0.23±0.09	0.00±0.00	0.00±0.00	0.00±0.00	0.00±0.00	0.00±0.00	0.00±0.00
PC	0.46±0.01	0.09±0.00	0.46±0.01	0.16±0.01	0.01±0.00	0.02±0.00	0.03±0.00	0.02±0.00	0.02±0.00	0.00±0.00
Sortnregress	0.63±0.00	0.21±0.00	0.63±0.00	0.29±0.00	0.00±0.00	0.07±0.00	0.25±0.00	0.07±0.00	0.11±0.00	0.01±0.00
GIES	0.52±0.01	0.11±0.00	0.52±0.01	0.19±0.00	0.01±0.00	0.02±0.00	0.04±0.00	0.02±0.00	0.02±0.00	0.00±0.00
DCDFG-MLP	0.40±0.01	0.04±0.01	0.40±0.01	0.11±0.01	0.00±0.00	0.07±0.01	0.07±0.03	0.07±0.01	0.07±0.02	0.00±0.00
DCDI-DSF	0.39±0.00	0.07±0.00	0.38±0.00	0.14±0.00	0.00±0.00	0.03±0.00	0.06±0.00	0.03±0.00	0.04±0.00	0.00±0.00
DCDI-G	0.44±0.02	0.12±0.00	0.44±0.02	0.18±0.00	0.00±0.00	0.02±0.00	0.06±0.00	0.02±0.00	0.03±0.00	0.00±0.00
Random (k=1000)	0.26±0.02	0.02±0.00	0.25±0.02	0.07±0.01	0.01±0.00	0.01±0.00	0.01±0.00	0.01±0.00	0.01±0.00	0.00±0.00

rankings. This ranking thus gives the same weight to each evaluation method. Results are summarized in Table 6 for the K562 cell line and in Table 7 for the RPE1 cell line.

## E Run time

We here present the average run time for each method in Table 8 for the K562 cell line and in Table 9 for the RPE1 cell line

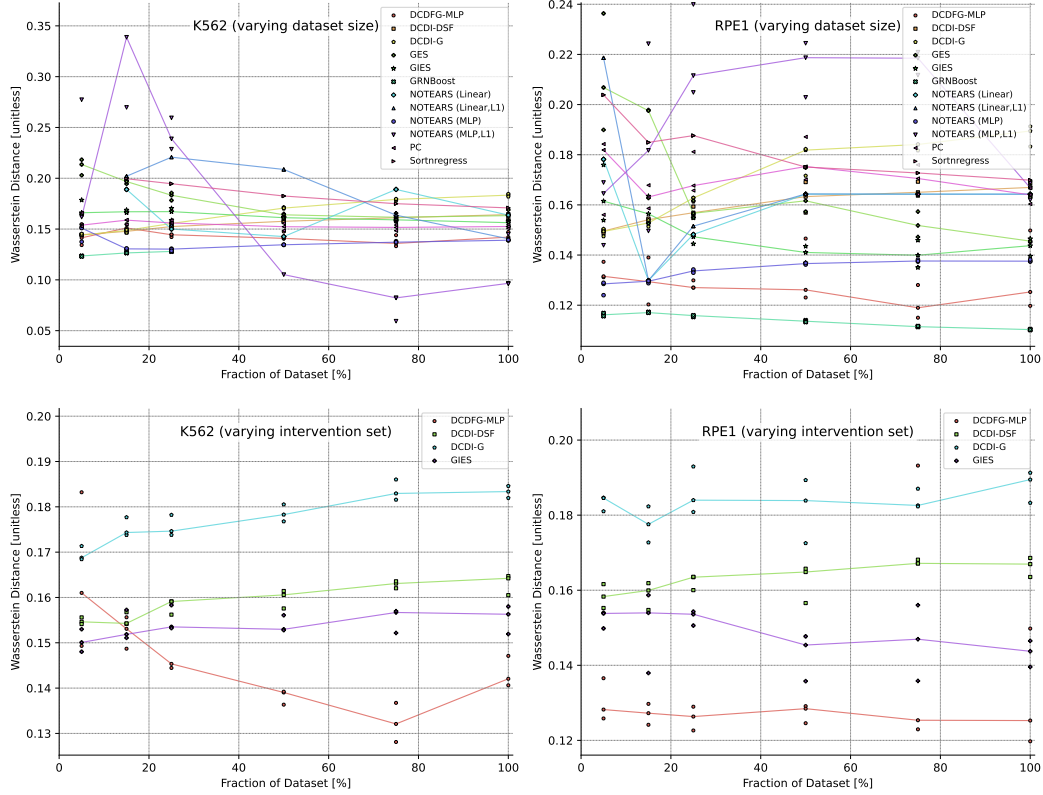


Figure 5: Performance comparison in terms of Mean Wasserstein Distance (unitless; y-axis) of 7 methods for causal graph inference on observational data (top row; (see legend top right) and 6 methods on interventional scRNAseq data (centre row; see legend centre right) when varying the fraction of the full dataset size available for inference (in %; x-axis), and 6 methods on interventional data (bottom row; see legend bottom right) when varying the fraction of the full intervention set used (in %, x-axis). Markers indicate the values observed when running the respective algorithms with one of three random seeds, and colored lines indicate the median value observed across all tested random seeds for a method.

Table 5: Partition sizes used for each model. -1 means that the graph was not partitioned.

Model name	partition size
PC	30
GES	30
GIES	30
NOTEARS (Linear)	-1
NOTEARS (Linear, L1)	-1
NOTEARS (MLP)	-1
NOTEARS (MLP, L1)	-1
DCDI-DSF	50
DCDI-G	50
DCDFG-MLP	-1
GRNBoost	-1
Sortnregress	-1

Table 6: Complete ranking on the K562 cell line.

Model	Rank Wasserstein	Rank FOR	Mean Rank	Wasserstein Distance	FOR
GRNBoost	12	1	6.500	0.133 ± 0.000	0.126 ± 0.000
DCDI-G	1	12	6.500	0.183 ± 0.001	0.182 ± 0.021
Sortnregress	2	12	7.000	0.171 ± 0.000	0.184 ± 0.000
DCDI-DSF	5	12	8.500	0.163 ± 0.003	0.181 ± 0.017
GES	5	12	8.500	0.164 ± 0.006	0.185 ± 0.025
NOTEARS (Linear)	5	12	8.500	0.164 ± 0.000	0.188 ± 0.027
GIES	7	12	9.500	0.155 ± 0.004	0.183 ± 0.025
PC	7	12	9.500	0.152 ± 0.002	0.187 ± 0.025
NOTEARS (MLP)	12	12	12.000	0.139 ± 0.000	0.179 ± 0.003
DCDFG-MLP	12	12	12.000	0.143 ± 0.004	0.180 ± 0.000
NOTEARS (Linear,L1)	12	12	12.000	0.140 ± 0.000	0.188 ± 0.027
NOTEARS (MLP,L1)	12	12	12.000	0.113 ± 0.032	0.188 ± 0.027

Table 7: Complete ranking on the RPE1 cell line.

Model	Rank Wasserstein	Rank FOR	Mean Rank	Wasserstein Distance	FOR
Sortnregress	2	3	2.500	0.170 ± 0.000	0.114 ± 0.000
GRNBoost	12	1	6.500	0.110 ± 0.000	0.110 ± 0.000
DCDI-G	1	12	6.500	0.188 ± 0.005	0.135 ± 0.007
NOTEARS (MLP)	11	3	7.000	0.138 ± 0.000	0.111 ± 0.012
PC	7	12	9.500	0.164 ± 0.004	0.131 ± 0.020
DCDI-DSF	7	12	9.500	0.166 ± 0.003	0.133 ± 0.007
NOTEARS (MLP,L1)	7	12	9.500	0.166 ± 0.004	0.138 ± 0.016
NOTEARS (Linear)	7	12	9.500	0.164 ± 0.000	0.138 ± 0.016
NOTEARS (Linear,L1)	7	12	9.500	0.164 ± 0.000	0.138 ± 0.016
DCDFG-MLP	11	12	11.500	0.132 ± 0.018	0.129 ± 0.009
GES	11	12	11.500	0.151 ± 0.012	0.133 ± 0.017
GIES	11	12	11.500	0.143 ± 0.004	0.140 ± 0.008

Table 8: Run time in wall clock hours for each method on the K562 cell line.

Model	Run time (hours)
GRNBoost	0.087988
Sortnregress	0.089441
GIES	0.653034
NOTEARS (MLP,L1)	1.526646
DCDI-DSF	1.586062
DCDFG-MLP	1.768952
PC	2.610882
GES	3.337906
DCDI-G	4.600406
NOTEARS (Linear,L1)	5.158183
NOTEARS (Linear)	5.814321
NOTEARS (MLP)	9.134294

Table 9: Run time in wall clock hours for each method on the RPE1 cell line.

Model	Run time (hours)
Sortnregress	0.045235
GRNBoost	0.058020
DCDI-DSF	0.494506
DCDFG-MLP	1.029798
GIES	1.082506
NOTEARS (MLP,L1)	1.116924
GES	1.333881
DCDI-G	1.793924
NOTEARS (Linear)	1.807665
NOTEARS (Linear,L1)	1.821760
PC	5.610735
NOTEARS (MLP)	8.455514